



Heriot-Watt University

Heriot-Watt University  
Research Gateway

## Noise suppression using optimum filtering of OCs generated by a multiport encoder/decoder

Kodama, Takahiro; Wada, Naoya; Cincotti, Gabriella; Wang, Xu; Kitayama, Ken-ichi

*Published in:*  
Optics Express

*DOI:*  
[10.1364/OE.20.010320](https://doi.org/10.1364/OE.20.010320)

*Publication date:*  
2012

[Link to publication in Heriot-Watt Research Gateway](#)

*Citation for published version (APA):*

Kodama, T., Wada, N., Cincotti, G., Wang, X., & Kitayama, K. (2012). Noise suppression using optimum filtering of OCs generated by a multiport encoder/decoder. *Optics Express*, 20(9), 10320-10329. [10.1364/OE.20.010320](https://doi.org/10.1364/OE.20.010320)



# Noise suppression using optimum filtering of OCs generated by a multiport encoder/decoder

Takahiro Kodama,<sup>1\*</sup> Naoya Wada,<sup>2</sup> Gabriella Cincotti,<sup>3</sup> Xu Wang,<sup>4</sup> and Ken-ichi Kitayama<sup>1</sup>

<sup>1</sup>Department of Electrical Electronic, and Information Engineering, Osaka University, 565-0871 Osaka, Japan

<sup>2</sup>Ultrafast Photonic Network Group, National Institute of Information and Communication Technology, 184-8795 Tokyo, Japan

<sup>3</sup>Department of Applied Electronics, University Roma Tre, via della Vasca Navale 84, I-00146 Rome, Italy

<sup>4</sup>School of Engineering and Physical Sciences, Heriot-Watt University, Riccarton, EH14 4AS, Edinburgh, UK  
[\\*kodama@pn.comm.eng.osaka-u.ac.jp](mailto:kodama@pn.comm.eng.osaka-u.ac.jp)

**Abstract:** We propose a novel receiver configuration using an extreme narrow band-optical band pass filter (ENB-OBPF) to reduce the multiple access interference (MAI) and beat noises in an optical code division multiplexing (OCDM) transmission. We numerically and experimentally demonstrate an enhancement of the code detectability, that allows us to increase the number of users in a passive optical network (PON) from 4 to 8 without any forward error correction (FEC).

©2012 Optical Society of America

**OCIS codes:** (060.4230) Multiplexing; (060.4510) Optical communications; (080.1238) Array waveguide devices.

---

## References and links

1. K. Kitayama and M. Murata, "Versatile optical code-based MPLS for circuit, burst, and packet switchings," *J. Lightwave Technol.* **21**(11), 2753–2764 (2003).
2. N. Kataoka, N. Wada, G. Cincotti, K. Kitayama, and T. Miyazaki, "A novel multiplexed optical code label processing with huge number of address entry for scalable optical packet switched network," ECOC 2007, Tu.3.2.3, Berlin, Germany, Sep. 2007.
3. P. R. Prucnal, *Optical Code Division Multiple Access: Fundamentals and Applications* (Taylor Francis Inc, 2005).
4. G. Cincotti, N. Wada, and K. Kitayama, "Characterization of a full encoder/decoder in the AWG configuration for code-based photonic routers—part I: modeling and design," *J. Lightwave Technol.* **24**(1), 103–112 (2006).
5. X. Wang and K. Kitayama, "Analysis of beat noise in coherent and incoherent time-spreading OCDMA," *J. Lightwave Technol.* **22**(10), 2226–2235 (2004).
6. S. Etemad, T. Banwell, S. Galli, J. Jackel, R. Menendez, P. Toliver, J. Young, P. Delfyett, C. Price, and T. Turpin, "Optical-CDMA incorporating phase coding of coherent frequency bins: concept, simulation, experiments," OFC 2004, FG5, LA, CA, USA, Feb. 2004.
7. H. Sotobayashi, W. Chujo, and K. Kitayama, "1.6-b/s/Hz 6.4 Tb/s QPSK-OCDM/WDM (4OCDM x WDM x 40Gb/s) transmission experiment using optical hard thresholding," *IEEE Photon. Technol. Lett.* **14**(4), 555–557 (2002).
8. J. H. Lee, P. C. Teh, P. Petropoulos, M. Ibsen, and D. J. Richardson, "Reduction of interchannel interference noise in a two-channel grating-based OCDMA system using a nonlinear optical loop mirror," *IEEE Photon. Technol. Lett.* **13**(5), 529–531 (2001).
9. Z. Jiang, D. S. Seo, S. D. Yang, D. E. Leaird, R. V. Roussev, C. Langrock, M. M. Fejer, and A. M. Weiner, "Four user, 2.5-Gb/s, spectrally coded OCDMA system demonstration using low-power nonlinear processing," *J. Lightwave Technol.* **23**(1), 143–158 (2005).
10. T. Hamanaka, X. Wang, N. Wada, A. Nishiki, and K. Kitayama, "Ten-user truly asynchronous gigabit OCDMA transmission experiment with a 511-chip SSFBG en/decoder," *J. Lightwave Technol.* **24**(1), 95–102 (2006).
11. G. Manzacca, M. S. Moreolo, and G. Cincotti, "Performance analysis of multidimensional codes generated/processed by a single planar device," *J. Lightwave Technol.* **25**(6), 1629–1637 (2007).
12. N. Kataoka, N. Wada, X. Wang, G. Cincotti, A. Sakamoto, Y. Terada, T. Miyazaki, and K. Kitayama, "Field trial of duplex, 10Gbps x 8-user DPSK-OCDMA system using a single 16 x 16 multi-port encoder/decoder and 16-level phase-shifted SSFBG encoder/decoders," *J. Lightwave Technol.* **27**(3), 299–305 (2009).
13. S. Yoshima, N. Nakagawa, N. Kataoka, N. Suzuki, M. Noda, M. Nogami, J. Nakagawa, and K. Kitayama, "10Gb/s-based PON over OCDMA uplink burst transmission using SSFBG encoder/multi-port decoder and burst-mode receiver," *J. Lightwave Technol.* **28**(4), 365–371 (2010).
14. S. Yoshima, Y. Tanaka, N. Kataoka, N. Wada, J. Nakagawa, and K. Kitayama, "Full-duplex 10G-TDM-OCDMA-PON system using only a pair of en/decoder," ECOC 2010, Tu.3.B.6, Torino, Italy, Sep. 2010.
15. X. Wang, N. Wada, G. Cincotti, T. Miyazaki, and K. Kitayama, "Demonstration of over 128-Gb/s-capacity (12-

- user/spl times/10.71-Gb/s/user) asynchronous OCDMA using FEC and AWG-based multiport optical encoder/decoders," *IEEE Photon. Technol. Lett.* **18**(15), 1603–1605 (2006).
16. G. Manzacca, A. M. Vegni, X. Wang, N. Wada, G. Cincotti, and K. Kitayama, "Performance analysis of a multiport encoder/decoder in OCDMA scenario," *IEEE J. Sel. Top. Quantum Electron.* **13**(5), 1415–1421 (2007).
- 

## 1. Introduction

Optical code (OC) processing is a flexible all optical technique that can overcome the electronic bottleneck in high speed packet switching networks, since optical labels are not related to physical resources and are generated and processed directly in the optical domain [1,2]. OCs are also used in OCDM systems to provide scalable asynchronous access to a large number of users. Whereas 10 Gbps time division multiplexing (TDM)-based PON (10G-PON) is the technology for the next generation access networks (NGAN), and the corresponding standardization activities have been already completed in IEEE802.3av and ITU-T G.984.5, OCDM technique is considered one of the possible candidates for future next generation PON (NG-PON2) systems, as it presents unique features, such as high data confidentiality, soft capacity on demand and possible quality of service (QoS) management [3].

During the past decade, coherent OCs, where the encoding information is embedded in the phases of the OC spectrum and/or time chips, have been largely investigated in literature, as they present enhanced correlation properties, with respect to incoherent OCs, and larger spectral efficiency. Novel coherent time-spreading (TS) encoding systems have been demonstrated using only compact optical passive devices, a planar cost-effective multiport device has been designed and its prototypes have been used in many different packet switching and OCDM experiments. The multiport encoder/decoder (E/D) has the unique capability of simultaneously generating/processing multiple phase shift keying (PSK) OCs [4].

In OCDM coherent systems, MAI and beat noises are the main issues that limit the system performance and many techniques have been proposed to overcome these impairments [5]. The spectral amplitude of conventional TS OCs, using for instance M-sequence or Gold codes, is almost constant over a broad interval of frequencies (as shown in Fig. 1), so that the pulse width of autocorrelation signal is only a few picoseconds large; in this case, it is possible to reduce the influence of MAI and beat noises by using optical time gating [6,7] and optical thresholding [8–10]. On the other hand, the width of the autocorrelation signal of the PSK OCs generated by a multiport E/D is much broader and smoother, and it is not possible to use optical thresholding, unless we do not refer to a complete synchronous transmission.

The spectral content of PSK OCs generated by the multiport E/D is equivalent to a single Fourier subcarrier of an orthogonal frequency division multiplexing (OFDM) signal and the corresponding orthogonality properties stems from the fact that the subcarriers have almost non-overlapping frequency spectra. The frequency crosstalk between two subcarriers is related to the MAI noise and affects the OC detection parameter. The PSK OCs generated at adjacent ports of the multiport E/D have partially overlapping spectra and the largest frequency crosstalk [4,11]; this impairment has been the main reason why in all our previous experiments, we were not able to fully exploit the encoding/decoding capabilities of the device, using all the device ports.

To increase the number of the available OCs, in this paper we introduce a new filtering technique based on an ENB-OBPF, that reduces the crosstalk and enhances the OC recognition parameter. We present both numerical simulations and experimental validations that demonstrate the reduction of MAI and beat noises. We also analyze the performance of a 10 Gbps, OCDMA-based PON system using paired multiport E/Ds, comparing the bit error rate (BER) performances for the cases when the ENB-OBPF is used or not. Opposite to a conventional OFDM system that uses the same multiport E/D, all our previous and present OCDM experiments have been always characterized by a fully asynchronous transmission, that is a key feature for the next generation access systems.

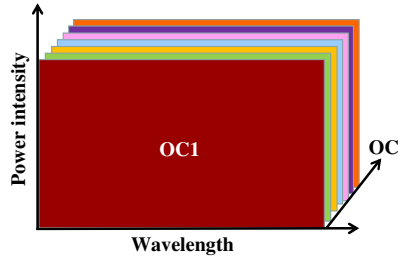


Fig. 1. Conventional TS-OC spectrums.

## 2. Analysis of the code detection performance

### 2.1 Numerical simulations

To evaluate the code detection performances, we have analyzed three different systems: without any filter, using a rectangular profile ENB-OBPF and with an ENB-OBPF obtained with an apodized fiber Bragg grating (FBG), as shown in Fig. 2(a). The bandwidths of the rectangular and apodized filters have been chosen to fit with the main lobe of the autocorrelation spectrum (see Fig. 2(b)). The channel spacing of a 16-port device with 200GHz free spectral range (FSR) is 0.1nm, that almost equates the main lobe width of the autocorrelation spectrum [4]. The choice of an apodized FBG relies on its enhanced filtering features, with respect to standard FBG filters; also this device allows a flexible design of the optical transfer function and it is extremely compact so that it can be easily placed at the RN and OLT. The transfer function of apodized FBG filter is shown in Fig. 2(b). Figure 2(c) shows the architecture used to numerically evaluate the code performance: a 2ps pulse from a mode locked laser diode (MLLD) is sent to an optical switch (SW) that selects the input port  $k$  of the encoder. At the receiver output  $k'$ , we measure the autocorrelation signal if  $k' = k$ , otherwise we detect the crosscorrelation signals. The two main parameters used to evaluate the system performance are the power contrast ratio (PCR) [12], i.e. the ratio between the average power of autocorrelation and crosscorrelation waveforms, and the ratio between the autocorrelation and crosscorrelation (ACP/CCP) peaks [4,11]. Using the formulas of Refs [4,11,12], we have calculated the PCR and ACP<sup>2</sup>/CCP<sup>2</sup> ratio for different bandwidth values and different filtering shapes of the ENB-OBPF, that are shown in Fig. 3: we observe that the rectangular filter removes a large part of the autocorrelation signal. On the other hand, the apodized FBG filter has a narrower filter shape that better fits with the autocorrelation spectrum; at the same time, the FBG filter more efficiently eliminates the outband MAI.

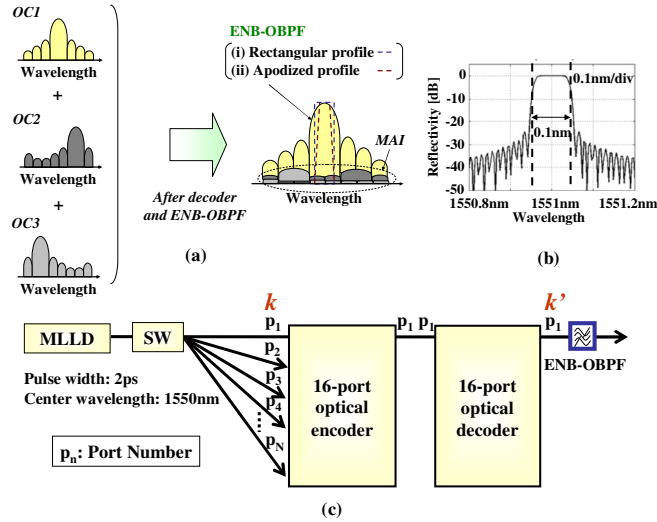


Fig. 2. (a) Filtering characteristics of two ENB-OBPFs, with rectangular and apodized profile (b) Apodized filter shape (c) Architecture to evaluate the OC detection performance.

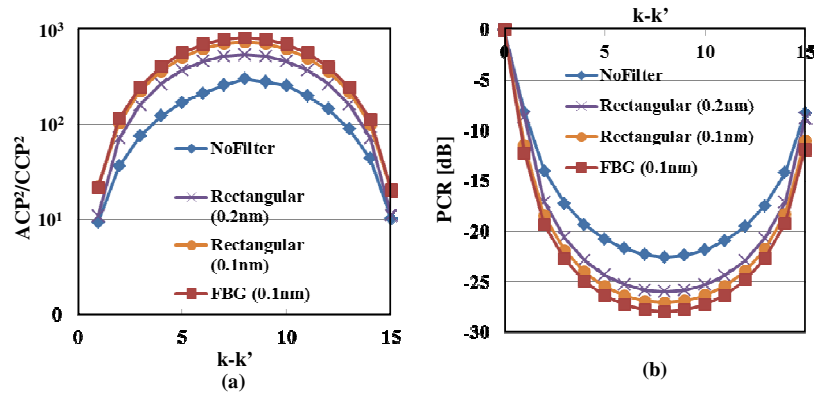


Fig. 3. (a)  $ACP^2/CCP^2$  at the decoder output #1 (b) PCR at the decoder output #1.

## 2.2 Experimental validation

Figure 4 shows the experimental setup that we used to evaluate the MAI and beat noise effects. The MLLD at 1550 nm is driven at 9.95328 GHz and the pulse stream is down-converted to 622.08 MHz by a LN-IM, to reduce the bit rate and completely eliminate the inter symbol interference (ISI). The OBPF after LN-IM is used only to remove the amplified spontaneous emission (ASE) noise. A 3 dB coupler splits the bit stream in two signals, that are forwarded to the ports #1 and #3 of a 16x16 multiport E/D. Each PSK OCs is composed of 16 chips with 200 Gchip/s rate. By using two switches (SW), it has been possible to transmit a single OC or two OCs simultaneously, to measure the autocorrelation and the cross-correlation signals, respectively. In addition, the polarization controllers (PC) and the polarizers (Pol) were used to investigate the system performance in the worst case scenario, when the polarization states of two OCs are aligned.

At the receiver side, the signal is sent to a multiport E/D, and the output #1 is connected to an ENB-OBPF with 0.1 nm bandwidth at the center wavelength of 1551 nm, in the case of evaluation of the performance with a filter, or connected directly to the monitoring system. The resolutions of the optical spectrum analyzer are used 1 nm/div and 0.1 nm/div.

Insets (i, ii) of Fig. 4 show the cases without any filter and with the ENB-OBPF, respectively; The measured autocorrelation and the cross-correlation waveforms are shown in insets (a, b), respectively and they have the same scales, and insets (c, d) show the autocorrelation waveform when both OCs are transmitted, and the corresponding spectrum. An inspection of these figures confirms that the use of an ENB-OBPF largely reduces the MAI and beat noise effect. To increase the receiver sensitivity, it is necessary to filter the outband MAI noise, without degrading the autocorrelation signal; for this reason, a tradeoff is required: the apodized filter shape and width has been selected to fit with the main lobe of the autocorrelation signal, where the large part of the power of the matched signal is comprised.

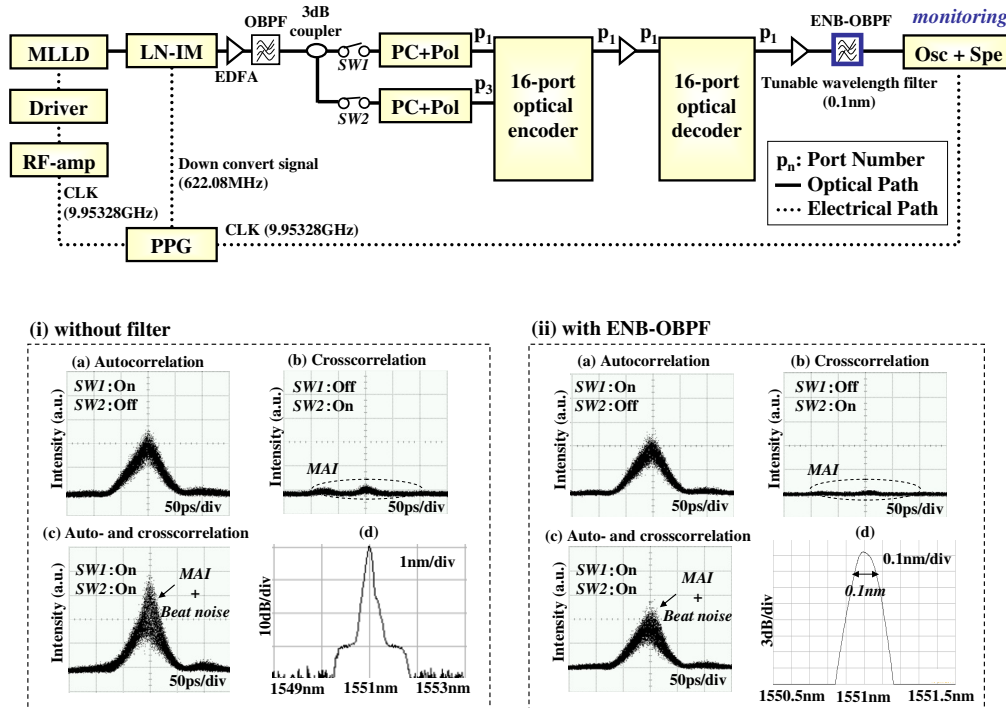


Fig. 4. Experimental setup and results.

### 3. Analysis of the system performance of a 10 Gbps, OCDM-PON

#### 3.1 System configuration

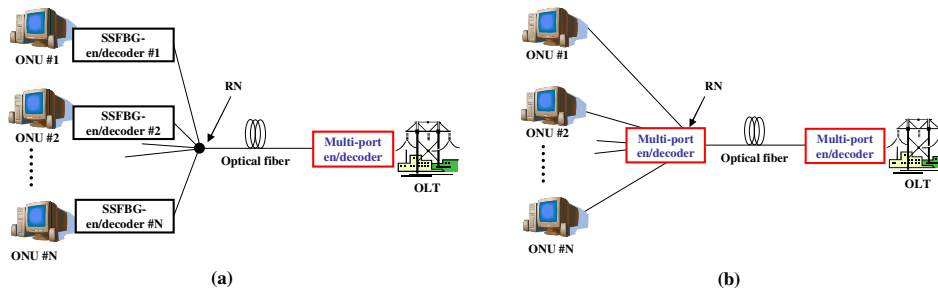


Fig. 5. (a) OCDM-based PON using hybrid E/D system (b) System with paired multipoint E/D.

In our previous experiments, we have used both a multipoint E/D and phase-shifted superstructured fiber Bragg grating (SSFBG) E/Ds, that can generate a single PSK OC. The

use of the multiport E/D is cost effective in the optical line terminal (OLT), where all the OCs must be generated and processed, whereas the SSFBG E/Ds are suitable for the optical network units (ONU) because they present polarization independent performance, low and code-length independent insertion losses, compactness as well as low cost for mass production. Recently, we have designed and fabricated new apodized SSFBG E/Ds to enhance the uplink performance of an OCDM system with a hybrid configuration [12, 13], that is shown in Fig. 5(a). However, this system does not satisfy the colorless (non-user specific) condition for ONUs, because each user terminal requires a different device. To overcome this limitation, we have proposed and demonstrated PON configurations with paired multiport E/Ds, located at the OLT and in the remote node (RN), respectively [14], as shown in Fig. 5(b). Table 1 summarizes some recent experimental results of a 10 Gbps, OCDM-based PON systems using a 16x16 multiport E/D. In a paired multiport E/D system, we were able to transmit simultaneously signals from 12 users, using FEC [15]. The use of FEC was mandatory since a paired multiport E/D system does not present the same performances as a hybrid E/D system, due to the MAI and coherent beat noises. To increase the number of ONUs, we introduce the ENB-OBPF.

**Table 1. Latest Experimental Results of a 10Gbps OCDM-Based PON Systems Using a Multiport E/D**

System configuration	Data format	FEC	Achieved user number	Reference
Hybrid E/D	DPSK	O FF	8	[12]
	OO K	O FF	4	[13]
Paired multi-port E/D	OO K	O FF	4	[14]
	OO K	O N	12	[15]

### 3.2 Theoretical analysis

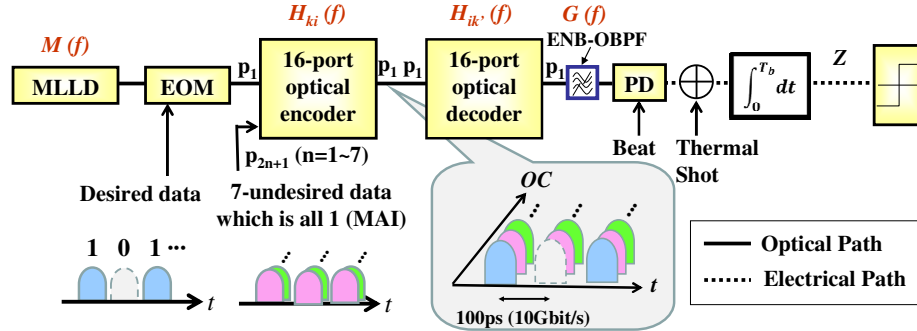


Fig. 6. Architecture to evaluate the performance of a 8 ONU, 10Gbps, OCDM-based PON.

To analyze the system performance, we have numerically investigated a 10Gbps, 8 ONUs, on-off keying (OOK) OCDM-based PON system with paired multiport E/Ds, using data rate detection. In this case, the 8 ports  $p_n = 2n-1$  ( $n = 1-8$ ) of a 16x16 multiport E/D are used, as shown in Fig. 6. Without considering dispersion effects, about 95% of the autocorrelation signal power of each bit is contained in one bit slot, so ISI effect is negligible. The autocorrelation signal  $E_{ac}(t)$  can be expressed as

$$E_{ac}(t) = \int_{-\infty}^{\infty} M(f)H_{ki}(f)H_{ik}^*(f)G(f)\exp(j2\pi ft)dt \quad (1)$$

where  $M(f)$  is the transfer function of the optical source,  $H_{ki}(f)$  and  $H_{ik'}(f)$  are the transfer functions of multipoint E/D, and  $G(f)$  is the transfer function of the ENB-OBPF. A similar expression can be obtained for the optical field of the crosscorrelation signal

$$E_{cc}(t) = \int_{-\infty}^{\infty} M(f)H_{ki}(f)H_{ik'}(f)G(f)\exp(\mathbf{j}2\pi f t) dt \quad (2)$$

with  $k' \neq k$ . The average power of the autocorrelation and crosscorrelation signals can be evaluated as

$$P_d = \int_0^{T_b} |E_{ac}(t)|^2 dt$$

$$P_i = \int_0^{T_b} |E_{cc}(t)|^2 dt \quad (3)$$

where  $T_b$  is the bit duration time. Considering the scheme of Fig. 6, the decision signal  $Z$  can be calculated as

$$Z = \Re P_d + \Re \sum_{i=2}^N P_i + 2\Re \sum_{i=2}^N \int_0^{T_b} |E_{ac}(t)| |E_{cc-i}(t)| \cos[\phi_{ac}(t) - \phi_{cc-i}(t)] dt$$

$$+ 2\Re \sum_{i=2}^N \int_0^{T_b} |E_{cc-i}(t)| |E_{cc-j}(t)| \cos[\phi_{cc-i}(t) - \phi_{cc-j}(t)] dt + n(t) \quad (4)$$

where  $\phi_{ac}$  is the phase of the autocorrelation signal,  $E_{cc-i} \exp(\phi_{cc-i})$  and  $E_{cc-j} \exp(\phi_{cc-j})$  are the interfering signals, and  $\Re$  is the photodetector responsibility and  $n$  is the Gaussian random signal, due to thermal and shot noises. In this expression, the first term is the matched signal, the second one is the MAI noise, the third and the fourth terms are the first and the second-order beat noises, respectively. The phase of the beat noise term is a random process; in our numerical evaluations, we considered only the first beat noise, assuming a Gaussian statistics, because the second beat noise does not affect the detection [16]. To investigate the system performance in the worst-case scenario, with the largest values of the MAI and beat noises, we assume that all the users are transmitting simultaneously and synchronously a logic “1”, except for desired ONU, that transmits both “0” and “1”. We also assume that all the signals have the same polarization. The beat noise variance has the following expression:

$$\sigma_{beat}^2 = \frac{\Re^2}{\pi} \sum_{i=2}^N \int_0^{2\pi} \int_0^{T_b} E_{ac}^2(t) E_{cc-i}^2(t) \cos^2 \theta_i dt d\theta_i \quad (5)$$

where  $\theta_i$  is a random variable with a uniform distribution between 0 and  $2\pi$ .  $\sigma_0^2$  and  $\sigma_1^2$  are the total noise variance corresponding to logic bits “0” and “1”, respectively

$$\sigma_0^2 = \sigma_{th}^2 + \sigma_{MAI}^2$$

$$\sigma_1^2 = \sigma_{beat}^2 + \sigma_{sh}^2 + \sigma_{MAI}^2 \quad (6)$$

and  $\sigma_{th}^2$ , and  $\sigma_{sh}^2$  are the thermal and shot noise variances, respectively

$$\sigma_{th}^2 = \frac{4k_B T B_R}{R_L}$$

$$\sigma_{sh}^2 = 2eB_R \Re P_d \left( 1 + \sum_{i=1}^m \frac{P_i}{P_d} \right) \quad (7)$$

Here  $k_B$  is Boltzmann constant,  $T$  is the temperature,  $B_R$  is the receiver bandwidth,  $e$  is the electron charge, and  $R_L$  is the load resistance. If the power level received at the PD is low,  $\sigma_{th}^2$



is dominant, and increasing the power,  $\sigma_{beat}^2$  of “1” transmission becomes dominant. Therefore, the beat and shot noises which are generated by MAI can be neglected for the case data “0” transmission. The error probabilities for an incorrect recognition are

$$Pe(1|0) = \frac{1}{2} \operatorname{erfc} \left[ \frac{\Re P_d \left( I_{th} - \sum_{i=2}^N \frac{P_i}{P_d} \right)}{\sqrt{2}\sigma_0} \right]$$

$$Pe(0|1) = \frac{1}{2} \operatorname{erfc} \left[ \frac{\Re P_d \left( 1 + \sum_{i=2}^N \frac{P_i}{P_d} - I_{th} \right)}{\sqrt{2}\sigma_1} \right]$$
(8)

where  $I_{th}$  is the detection threshold, and the BER is given by

$$BER = \Pr(0)_{data} Pe(1|0) + \Pr(1)_{data} Pe(0|1)$$

$$= \frac{1}{4} \left( \operatorname{erfc} \left[ \frac{\Re P_d \left( I_{th} - \sum_{i=2}^N \frac{P_i}{P_d} \right)}{\sqrt{2}\sigma_0} \right] + \operatorname{erfc} \left[ \frac{\Re P_d \left( 1 + \sum_{i=2}^N \frac{P_i}{P_d} - I_{th} \right)}{\sqrt{2}\sigma_1} \right] \right)$$
(9)

where  $\Pr(0)_{data}$ , and  $\Pr(1)_{data}$  are the probability of transmitting “0” or “1”.

### 3.3 Comparison of BER performances

**Table 2. Parameters Used in the Numerical Simulations**

Symbol	Value
$k_B$	$1.38 \times 10^{-23}$ J/K
$T$	300K
$B_R$	8.5 GHz
$R_L$	50 $\Omega$
$e$	$1.6 \times 10^{-19}$
$\Re$	0.85 A/W

We have numerically evaluated the BER in an OCDM-based PON system for different numbers of simultaneous users, without any filter and using the parameters reported in Table 2. The results are shown in Fig. 7 shows that the influence of the beat noise is highly dependent on the number of ONUs and that error-free ( $BER = 10^{-9}$ ) transmission can be achieved with only 4 simultaneous ONUs, as it has been also demonstrated in our previous experiments. In fact for 5 ONUs, the BER shows an error floor. The influence of the ENB-OBPF on the BER performance is illustrated in Fig. 8, where 8 ONUs have been considered: it is evident that in this case it is possible to achieve error-free transmission. We also observe that reducing the filter bandwidth filter to 0.1 nm enhances the BER performance, that can be further increased using an apodized profile. Figure 9 shows the power penalty ( $BER = 1 \times 10^{-9}$ ) for all the cases examined.

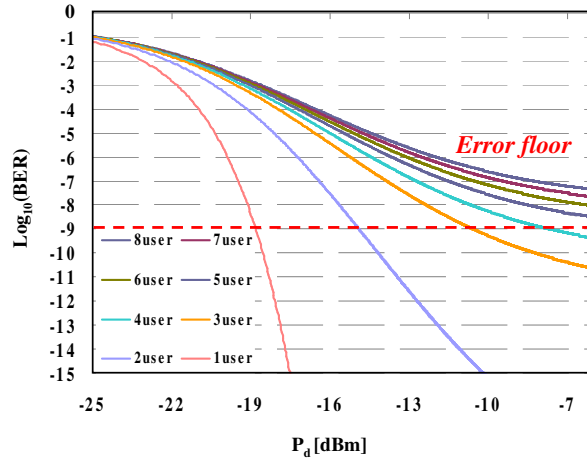


Fig. 7. BER performance of a conventional OOK-OCDM system with paired multiport E/D (without filter).

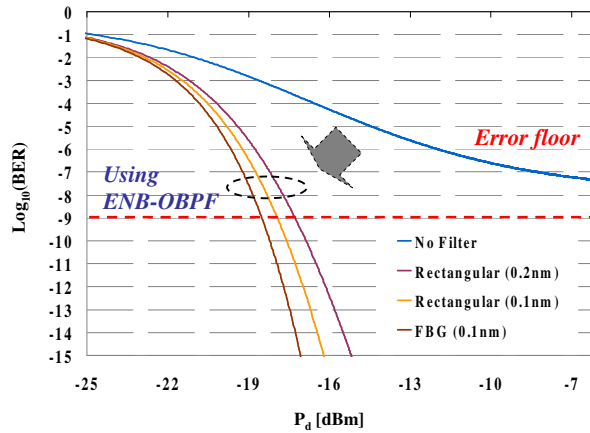


Fig. 8. BER performance using an ENB-OBPF.

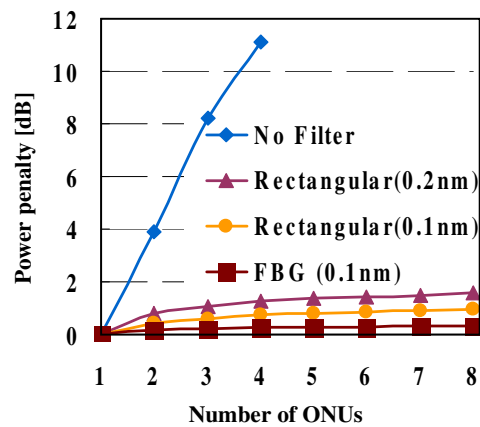


Fig. 9. Power penalty versus the number of ONUs.

#### **4. Conclusions**

We have demonstrated that an optimum filtering of the OC generated by a multiport E/D allows us to largely reduce the MAI and beat noise effects in label processing and OCDM transmission, with a drastic improvement of the code detection performance. We have also shown that this new architecture allows us to increase from 4 to 8 the number of simultaneous ONUs transmitting in a 10 Gbps OCDM-based PON, based on paired multiport E/Ds. The proposed technique can also be used to enhance the performances of systems with larger bit rate.

#### **Acknowledgment**

The authors would like to thank B. Dai of Heriot-Watt University for his kind cooperation. X. Wang acknowledges the support of Royal Society International Joint Project. This work was also supported by the Osaka University Scholarship for Short-term Overseas Research Activities 2011.